

A Novel Pseudocapacitance Mechanism of Elm Seeds-like Mesoporous

MoO_{3-x} Nanosheets as electrode for supercapacitor

Qian-Long Lu^{a,b}, Shi-Xi Zhao^{a*}, Chang-Ke Chen^{a,b}, Xia Wang^{a,b}, Yu-Feng Deng^a, Ce-Wen Nan^b

^aGraduate School at Shenzhen, Tsinghua University, Shenzhen, 518055, China

^bSchool of Materials Science and Engineering, Tsinghua University, Beijing, 100084, China

*Corresponding Author: Tel.: +86 0755 26036372; fax: +86 0755 26036372

E-mail: zhaosx@sz.tsinghua.edu.cn (Shi-Xi Zhao).

Supplementary figures and tables

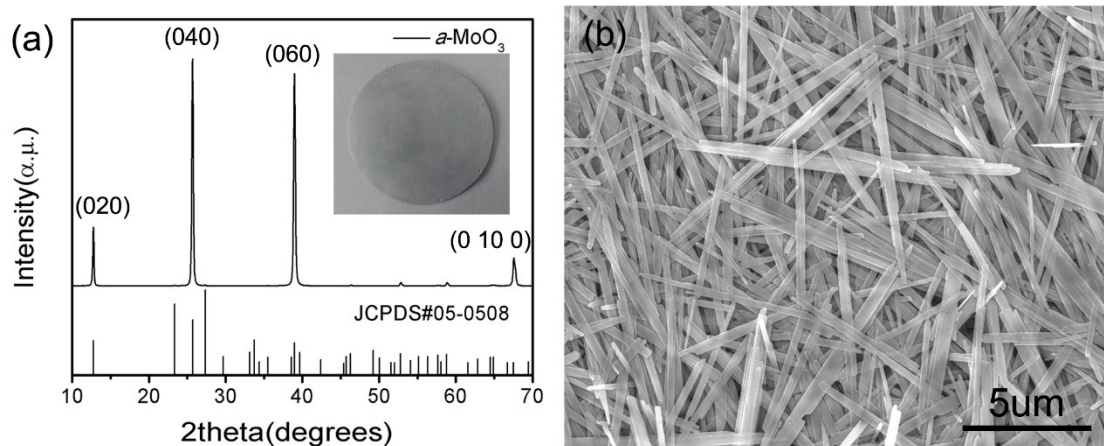


Fig. S1 (a) XRD pattern and color, (b) SEM image of generally synthesized α - MoO_3 nanobelts.

In the most works of α - MoO_3 based supercapacitors, α - MoO_3 was synthesized to be nanobelts and was white or light gray.¹⁻⁵ Because of the lamer crystal structure and obvious orientation, the diffraction peaks that corresponds the crystal face $\{0\ b\ 0\}$ ($b=2, 4, 6, 10$) are very intense. We also synthesized α - MoO_3 by a facile hydrothermal method and its color is light gray (**Fig. S1a, b**).

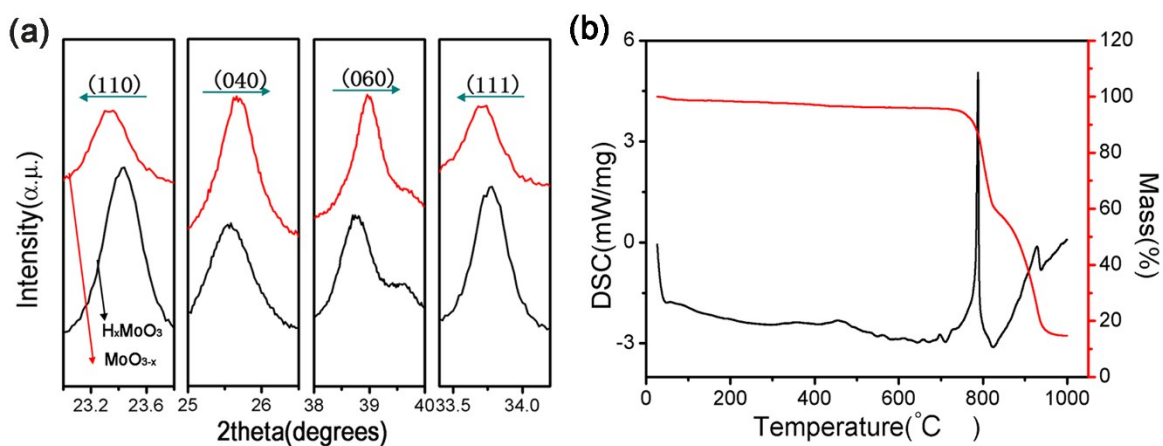
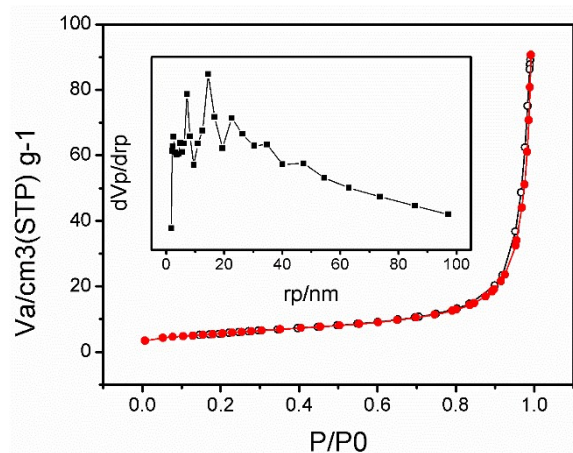


Fig. S2 (a) XRD peak position difference between H_xMoO_3 and MoO_{3-x} . (b) TAG-DSC curves of H_xMoO_3 in air.

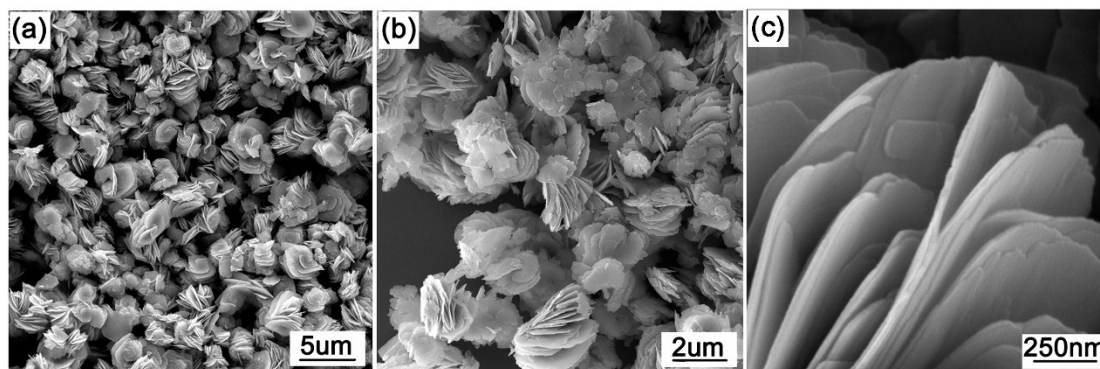
TAG-DSC curves of H_xMoO_3 indicate that its thermo-stability is high and it start smelting at around 800°C. Moreover, this also confirms there are no crystal water in H_xMoO_3 (**Fig. S2 (b)**).

Table S1. Integral area and percentage of every peak in XPS spectra.

	Int Area of P1	Int Area of P2	Int Area of P3	Int Area of P4
MoO_{3-x}	3867(4.4%)	45988(52.7%)	2631(3.0%)	34808(39.9%)
H_xMoO_3	2095(2.9%)	40145(55.7%)	1819(2.5%)	27957(38.9%)

**Fig. S3** N_2 adsorption–desorption isotherms and pore size distributions of H_xMoO_3 .**Table S2.** BET and BJH data of H_xMoO_3 and MoO_{3-x} .

	$a_{s,\text{BET}}$ ([$\text{m}^2 \cdot \text{g}^{-1}$])	Total pore volume($p/p_0=0.990$) [$\text{cm}^3 \cdot \text{g}^{-1}$]	Mean pore diameter [nm]
H_xMoO_3	20.17	0.13	25.77
MoO_{3-x}	22.48	0.145	25.86

**Fig. S4** Morphology of H_xMoO_3 obtained at different magnifications.

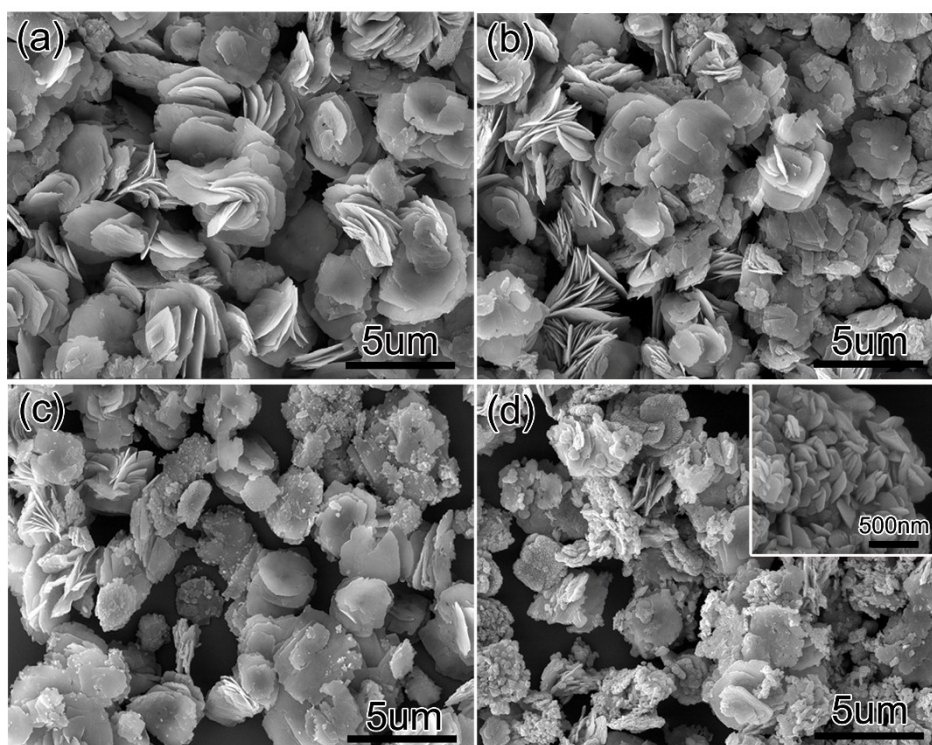


Fig. S5 The SEM images of the products of H_xMoO_3 hydrogenated at different temperatures (a)250°C; (b)300°C; (c)350 °C; (d)400 °C.

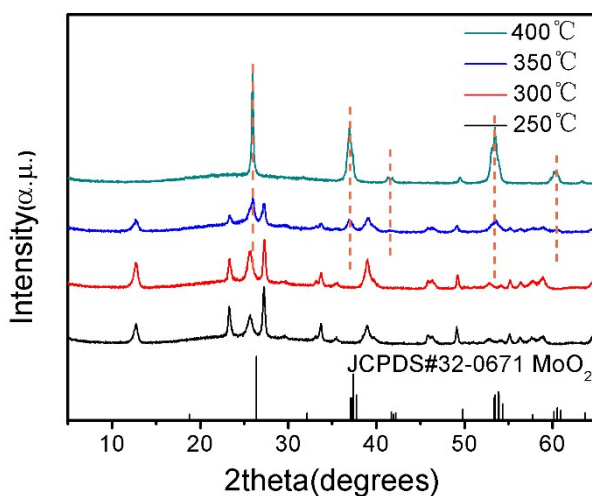


Fig. S6 XRD patterns of the products of H_xMoO_3 hydrogenated at different temperatures (a) 250°C; (b) 300 °C; (c) 350 °C; (d) 400 °C.

After hydrogenation at different temperatures, the morphology of the products took some changes. From 250 to 300°C, the main morphology remained unchanged except there are more random distributed nanoflakes. The XRD pattern of them were almost same and can be indexed to be α - MoO_3 . From 300 to 350°C, many nano-particles emerged on the surface of nanosheets. The peaks of α - MoO_3 and MoO_2

appeared in the pattern of sample 350°C at the same time. In combination the SEM images with XRD pattern, we can concluded that part of the α - MoO_3 was reduced to MoO_2 . From 350 to 400°C, the product changed significantly. Many nanosheets seems to split into nano-particles and the hierarchical structure disappeared.⁶ The sample 400°C can be indexed to be MoO_2 (Fig. S5, 6).

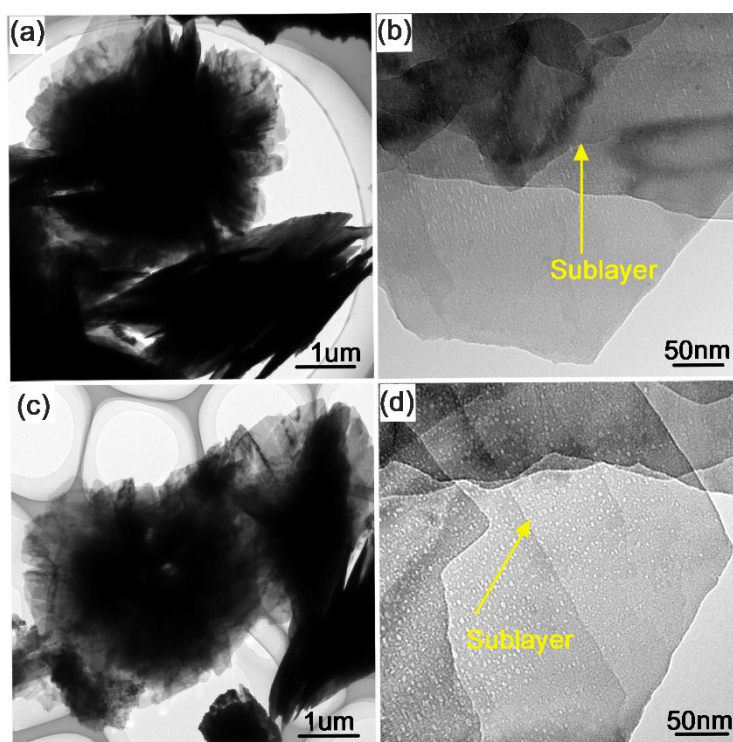


Fig. S7 TEM imagines of H_xMoO_3 (a), (b) and MoO_{3-x} (c), (d) obtained at different magnifications.

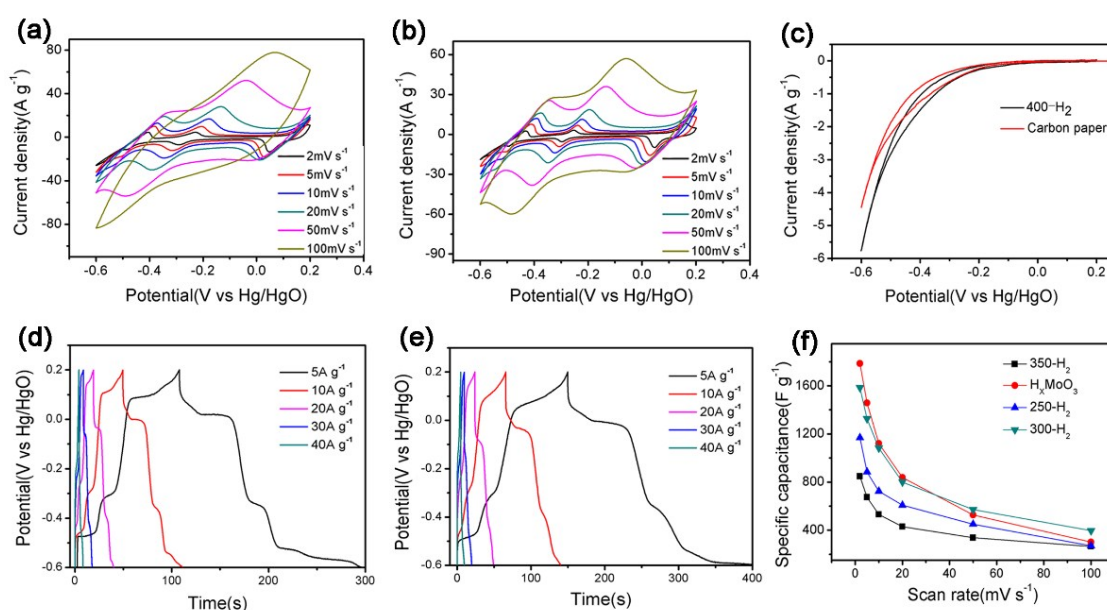


Fig. S8 CV curves of the hydrogenated products at (a) 250°C; (b)350°C; (c)400°C and carbon paper

current collector; (d) GCD curves of H_xMoO_3 and (e) MoO_{3-x} at different current densities; (f) specific capacitance at different scan rates of different hydrogenating products.

The products obtained at 250°C and 350°C could also deliver obvious pseudocapacitance like MoO_{3-x} and H_xMoO_3 , but the 400°C product shows no capacitive behavior because MoO_2 dissolved in H_2SO_4 electrolyte (Fig. S8.a, b, c). Among those products, the MoO_{3-x} (product of 300°C hydrogenation) shows best specific capacitance.

Specific capacitance C_s ($F \cdot g^{-1}$) of the electrodes were calculated from the CV and GCD curves by Eqs. (1) and (2), respectively, where I_1 (A) is the response current, ΔV_1 (V) is the potential window of electrodes, ΔV_2 (V) is the potential window without IR drop. v ($V \cdot s^{-1}$) is the scan rate, I_2 (A) is the constant discharge current, Δt_1 (s) is the discharging time and m (g) is the weight of the active material.

$$C_s = \frac{\int I_1 dv}{vm\Delta V_1} \quad (1)$$

$$C_s = \frac{I_2 \Delta t_1}{m\Delta V_2} \quad (2)$$

Specific capacitance C_a ($F \cdot g^{-1}$) of the asymmetric supercapacitor were calculated from the CV curves by Eqs. (3), where m_1 (g) and m_2 (g) is the weight of the active materials for positive and negative electrodes, ΔU (V) is potential window of asymmetric supercapacitor

$$C_a = \frac{\int I_1 dv}{v(m_1 + m_2)\Delta U} \quad (3)$$

The energy density (E ($W \cdot h \cdot kg^{-1}$)) and power density (P ($W \cdot kg^{-1}$)) of asymmetric supercapacitor can be calculated from C_a according to the following Eqs. (4) and (5), where Δt_2 (s) is the time calculated by $\Delta U/v$.

$$E = \frac{1}{2} \times 3.6 C_a \Delta U^2 \quad (4)$$

$$P = \frac{3600 E}{\Delta t_2} \quad (5)$$

Table S3. Electrical resistivity of α - MoO_3 , H_xMoO_3 , MoO_{3-x} .

Sample	Thickness(mm)	Diameter(mm)	electrical resistivity($\Omega \cdot cm$)
--------	---------------	--------------	---

$\alpha\text{-MoO}_3$	0.94	10.06	4.573×10^5
H_xMoO_3	0.62	10.06	1.082×10^3
MoO_{3-x}	0.64	10.06	7.882×10^{-2}

To detect the electrical resistivity of $\alpha\text{-MoO}_3$, H_xMoO_3 and MoO_{3-x} , the powder of them was pressed into disc. It is interesting to see that the electrical resistivity of H_xMoO_3 is smaller than that of $\alpha\text{-MoO}_3$.

The electrical conductivity of MoO_{3-x} was improved a lot after hydrogenation.

Table S4. Fitted impedance data obtained from Nyquist plots

	$R_s(\Omega)$	CPE	$R_{ct}(\Omega)$	W_d
MoO_{3-x}	1.84	2.75×10^{-3}	18.49	997.8
H_xMoO_3	2.47	1.16×10^{-3}	43.46	6970

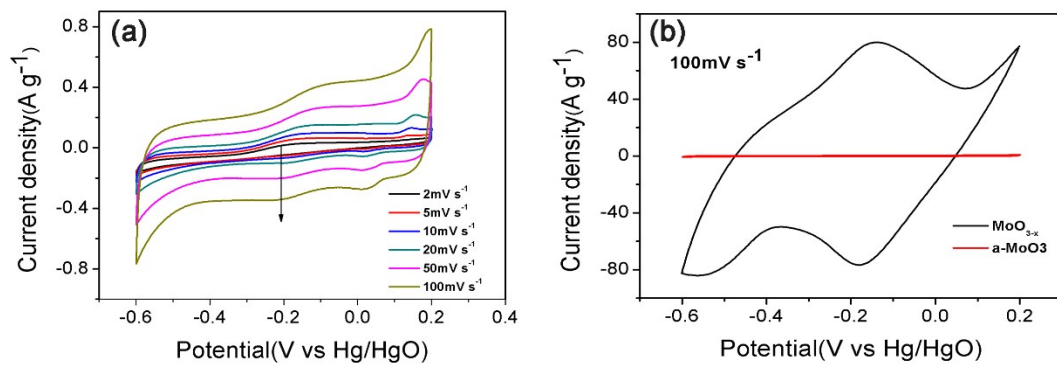


Fig. S9 (a) CV curves of $\alpha\text{-MoO}_3$ electrode at different scan rates; (b) CV curves of $\alpha\text{-MoO}_3$ and MoO_{3-x} electrodes at the scan rate of 100mV s^{-1} .

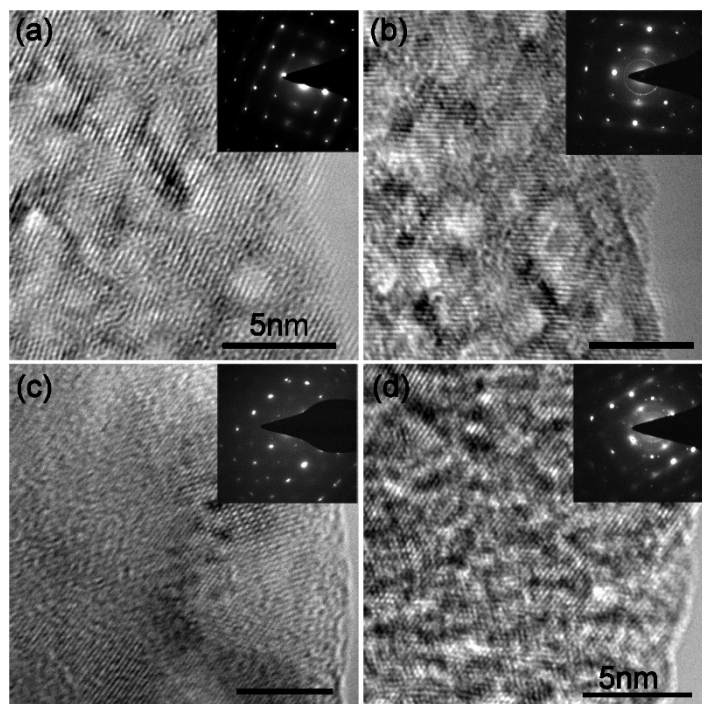


Fig. S10 HRTEM images of (a) H_xMoO_3 , (b) MoO_{3-x} (c) products of cycle 2 and d) cycle 10000. The insets show the corresponding SAED patterns.

- 1 L. Huang, X. Gao, Q. Dong, Z. Hu, X. Xiao, T. Li, Y. Cheng, B. Yao, J. Wan, D. Ding, Z. Ling, J. Qiu and J. Zhou, *J Mater Chem A*, 2015, **3**, 17217-17223.
- 2 B. Mendoza-Sanchez, T. Brousse, C. Ramirez-Castro, V. Nicolosi and P. S. Grant, *Electrochim Acta*, 2013, **91**, 253-260.
- 3 F. Wang, Z. Liu, X. Wang, X. Yuan, X. Wu, Y. Zhu, L. Fu and Y. Wu, *J Mater Chem A*, 2016, **4**, 5115-5123.
- 4 X. Xiao, Z. H. Peng, C. Chen, C. F. Zhang, M. Beidaghi, Z. H. Yang, N. Wu, Y. H. Huang, L. Miao, Y. Gogotsi and J. Zhou, *Nano Energy*, 2014, **9**, 355-363.
- 5 X. Xiao, C. Zhang, S. Lin, L. Huang, Z. Hu, Y. Cheng, T. Li, W. Qiao, D. Long, Y. Huang, L. Mai, Y. Gogotsi and J. Zhou, *Energy Storage Materials*, 2015, **1**, 1-8.
- 6 B. Hu, L. Q. Mai, W. Chen and F. Yang, *Acs Nano*, 2009, **3**, 478-482.